Available online at www.sciencedirect.com

SciVerse ScienceDirect

Ceramics International 38 (2012) 2347–2354

CERAMICS INTERNATIONAL

www.elsevier.com/locate/ceramint

Preparation, structural and microstructural properties of $Ba_{0.64}Ca_{0.32}Al_2Si_2O_8$ ceramics phase

A.S. Radosavljević-Mihajlović, M.D. Prekajski, J. Zagorac, A.M. Došen, S.S. Nenadović *, B.Z. Matović

Laboratory for Material Science, Institute for Nuclear Science Vinča, University of Belgrade, P.O. Box 522, 11001 Belgrade, Serbia

Received 15 August 2011; received in revised form 30 October 2011; accepted 31 October 2011
Available online 6 November 2011

Abstract

Monoclinic celsian has been prepared from Ba-LTA zeolite precursor. The Ca^{2+}-exchanged hexacelsian (HC_{Ca}) synthesized from Ba-LTA zeolite precursors was used for preparation of monoclinic celsian (MC_{Ca}). The partially ion exchange diphyllosilicate has a composition of $Ba_{0.64}Ca_{0.32}Al_2Si_2O_8$ (HC_{Ca}). It was found that prepared HC_{Ca} phase is stable between room temperature and 1300 °C. During prolonged heating this phase is polymorphic transformed to Ba, Ca-celsian feldspar. Synthesis of Ba, Ca-celsian and thermal behavior during transformation processes was observed by XRD method. The crystal structure and microstructural parameters were refined using Rietveld method. The crystal morphology of thermal treated samples was observed by SEM/EDAX analysis.

Keywords: Ceramics; Chemical synthesis; X-ray powder diffraction; Microstructure

1. Introduction

Barium aluminosilicates ($BaAl_2Si_2O_8$; BAS) exist in four different polymorphs. Monoclinic (S.G. *I*2/*c*) form named celsian (MC) is the most abundant material for a vast technological interest on account of its thermal and electrical properties; paracelsian (S.G. $P2_1/a$) and two synthetic forms are structural analogues of the two double-layer barium feldspar structure (PC), named α-hexacelsian (orthorhombic) and β-hexacelsian (hexagonal) (HC) [1–5]. Several methods have been used to synthesize MC ceramics: mixture of minerals [6], sol–gel processing [7,8], and thermally induced zeolite transformation [9–12]. However, some obstacles have been noticed in the process of synthesis of MC, which are related to the early crystallization of the HC polymorph. The HC polymorph is a precursor for the MC phase in all known syntheses. The spontaneous thermally induced transformation of HC → MC phase needs prolonged heating at temperatures higher than 1500 °C for several hours.

Several authors have observed the influence of various dopants on the acceleration of MC nucleation [13–20]. According to these results dopants have a significant role in accelerating of HC → MC transformation process. Dondur et al. [19,20] have noticed that the process of thermal transformation of HC → MC depends of the molar fractions of cations present in the structure of the starting precursors. On the other hand, Andreola et al. [21] showed that the optimum content of Na^+ is 0.43 mequiv./g which permits complete celsian crystallization at 1300 °C for 5 h. Lee et al. [17] investigated the influence of different dopant to the HC → MC transformation process. They concluded that the effect of dopants depends on the position and size of the cation in structure. For divalent cations, the effect of cationic size on promoting the conversion is as follows 0.99 Å (Ca^{2+}) > 0.66 Å (Mg^{2+}) > 1.12 Å (Sr^{2+}) > 0.35 Å (Be^{2+}). Bruno and Gazzoni [22] reported the study of the Ca–Ba diadochic substitution in the several polymorphic modification of $BaAl_2Si_2O_8$. Krzmanc et al. [23] investigated the substitution influence of Ba with Ca or Sr in $Sr_xBa_{1-x}Al_2Si_2O_8$–$Ca_xBa_{1-x}Al_2Si_2O_8$ solid solution. They find that the substitution with Ca-ion was more efficient in the hexacelsian-to-monocelsian transformation than a substitution with Sr-ion. However, the role of dopant is still not completely understood and how it was incorporated in the celsian crystal structure.

* Corresponding author..
E-mail address: msneza@vinca.rs (S.S. Nenadović).

0272-8842/$36.00
doi:10.1016/j.ceramint.2011.10.087

In this paper we show the results of thermally induced transformation of the partially ion exchanged diphyllosilicate phase (HC_{Ca}) into celsian. The celsian phase was obtained by a new chemical synthesis method. The motivations for this work were: (I) to observe the thermal behavior and to perform quantitative phase analysis of ion exchanged hexacelsian (HC_{Ca}) during the thermal transformation; (II) to determine the crystal structure of celsian with chemical composition $Ba_{0.64}Ca_{0.32}Al_2Si_2O_8$; and (III) to investigate the XRD pattern line broadening and influence of Ca^{2+} cation to microstructural parameters. The crystal structure and microstructural parameters of Ba, Ca-celsian was refined using the Rietveld method.

2. Experimental

The hexacelsian (HC) was synthesized by ZTIT procedure [24]. The sodium form of the LTA zeolite structure type [25] produced by The Union Carbide Corporation was used. The synthesized HC sample (chemical formula $BaAl_2Si_2O_8$) was used as a starting material for the further chemical modification.

The following procedure [26] was performed for the cation exchange of HC sample: 3 g of initial HC obtained in above described manner, was treated with 0.90 dm^3 of 0.21 M solution of $CaCl_2$ (solid/liquid ratio = 1/30) in autoclave near constant temperature of 180 °C. After 7 days the ion exchanged sample was washed thoroughly and dried at room temperature. The results of the chemical analysis show that the content of CaO in HC was 5.25 wt.%, suggesting that the Ca^{2+} for Ba^{2+} cation exchange was not completed (Table 1). In the HC sample prepared by the ion exchange method Ca^{2+} substituted Ba^{2+} up to ~40% and the sample was noted as HC_{Ca}. The presence of Si, Al, Na, Ca and Ba in the synthesized compounds was controlled using the EDAX method. The HC_{Ca} sample was thermally treated in the temperature range between 1000 and 1500 °C for 1 h. Transformation to monoclinic polymorph is completed at temperature 1500 °C. The results of atomic absorption spectrophotometer (ASS) using a Perkin-Elmer 390 spectrophotometer are shown in Table 1.

The XRD patterns were obtained on a Philips PW-1710 automated diffractometer using a Cu tube operated at 40 kV and 30 mA. The instrument is equipped with diffracted beam curved graphite monochromatic and a Xe-filled proportional counter. The diffraction data were collected in the range of 4–80° 2θ Bragg angles counting for 1 s at every 0.02°, for routine phase analysis. For a quantitative analysis of the X-ray powder diagrams Powder Cell 2.4 [27] software was used.

For the Rietveld profile fitting method the XRD data were collected using the step-scanning mode in the range between 4 and 135° 2θ with a 0.02° step and 12.5 s count time. Collected data were refined using the *FullProff* software [28]. The divergence and receiving slits were fixed at 1° and 0.1 mm, respectively. All the XRD measurements were performed *ex situ* at the room temperature in a stationary sample holder. To account for the instrumental broadening, the X-ray diffraction profile of a standard specimen CeO_2 was fitted by convolution to the experimental TCH pseudo-Voigt function [29].

The X-ray line broadening was calculated using Breadth software according to the Warren–Averbach and simplified integral breadth methods [30–33]. Input data for the Breadth program such as, unit-cell parameters, peak positions ($2\theta_{max}$) and Lorenz/Gauss mixing components (η), were taken from the output of the FullProf software. Microstructural parameters were observed for samples annealed at temperatures of 1420 and 1500 °C. The Rietveld refinement procedure was applied using the literature data for the celsian crystal structure [34].

Investigation of crystal morphology and chemical composition was carried out using LINK AN 1000 EDS microanalyses attached to a JEOL JSM-6460 LV scanning electron microscope. The ZAF-4/FLS software provided by LINK was used for corrections.

Table 1
The results of chemical analysis of ion exchanged hexacelsian and feldspar phase.

Sample	% SiO_2	%Al_2O_3	%BaO	%CaO	
HC	32.01	27.07	40.79	–	–
HC_{Ca}	34.90	29.67	28.45	5.25	–
MC_{Ca}	34.90	29.67	28.45	5.25	–
Results of EDX analysis					
	% Si	%Al	%Ba	%Ca	%O
HC_{Ca}	16.1	15.65	25.40	3.75	38.5
MC_{Ca}	15.93	15.65	25.40	3.75	37.6
Chemical formula of MC_{Ca} phase			$Ba_{0.64}Ca_{0.32}Al_2Si_2O_8$		

3. Results and discussion

3.1. Chemical and XRD analysis

Chemical composition of starting hexacelsian (HC), ion exchanged ($Ba^{2+} \rightarrow Ca^{2+}$) hexcelsian ($HC_{Ca}$) and feldspar phases (MC–Ca) are presented in Table 1. The EDS analyses are in good agreement with chemical analysis (Table 1).

According to the results of the chemical analysis (Table 1) it is clear that the percent of CaO in hexacelsian was 5.25%. After thermal treatment of the HC_{Ca} sample (1500 °C/1 h), the celsian phase was obtained, with following chemical composition $Ba_{0.64}Ca_{0.32}Al_2Si_2O_8$.

It is well-known that the framework of cation exchange zeolite collapses during heating treatment between 300 and 850 °C. Temperature when the zeolite network collapses depends on the Si/Al ratio, as well as the type and content of the extrafarmework cations. The formation of an amorphous phase in the Ba-LTA zeolite starts approximately between 400 and 600 °C, and the crystallization of hexacelsian occurs above 900 °C. During prolonged heating the polymorphic transforms of hexacelsian into celsian occurs. The process of recrystalization into a new phase depends mainly on the chemical properties of the extrafarmework and the modifier cations present in the observed system [9,35,36]. The literature data of the thermally induced phase transformation of M^{n+}-ion exchange hexacelsian are still unknown. The diffraction patterns of the thermally treated ion exchanged HC_{Ca} in temperature range of 1000–1500 °C are presented in Fig. 1.

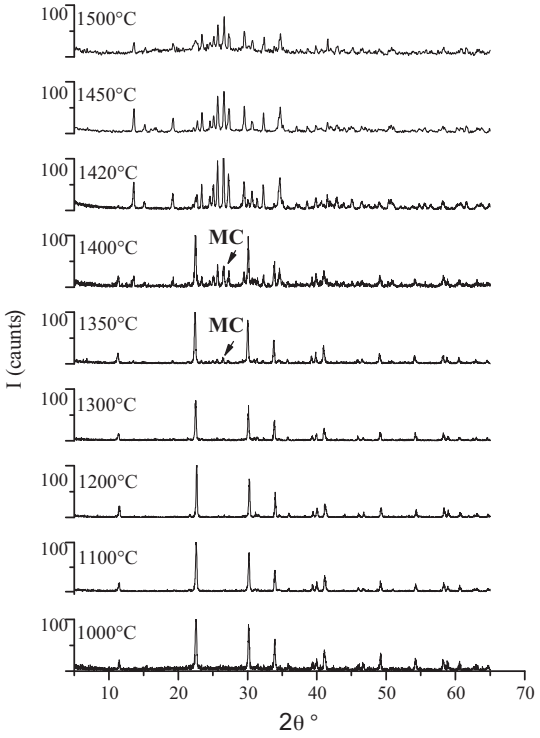

Fig. 1. Comparative XRPD-diagrams thermal treated samples HC_{Ca} in temperature range of 1000–1500 °C.

The change of the unit-cell parameters of the HC_{Ca} sample and quantitative phase analyses are presented in Table 2.

The ion-exchanged structure of hexacelsian (HC_{Ca}) is stable up to 1300 °C (Fig. 1 and Table 2). Prolonged heating treatment at 1350 °C, for 1 h, allows crystallization of small quantities of (14.6%) the celsian phase. According to the literature data [37] Ba-LTA zeolite completely recrystallizes into a monoclinic form $BaAl_2Si_2O_8$ after thermal treatment at 1100 °C/6 h and 1300 C/22 h. Furthermore, Ba-LTA zeolite (1.55% Na_2O) at annealing temperature 1300 °C/5 h shows the presence of the celsian phase (79.1%) and an amorphous phase of (20.8%) yielded Rietveld-RIR analysis [21]. The content of the celsian component increases with heating temperature in the HC_{Ca} sample (Fig. 1 and Table 2). After annealing at 1375 °C/1 h, the system consists of two phases: hexacelsian (∼54.7%) and celsian (∼45.3%) (Fig. 1 and Table 2). Thermal treatment of HC_{Ca} sample at 1420 °C for 1 h, results in crystallization of celsian phase in amount to 95.4% (Fig. 1 and Table 2). In the process of polymorphic transformation of ion exchanged HC_{Ca} hexacelsian it completely recrystalizes to celsian at 1500 °C/1 h temperature.The monoclinic form shows slight unit-cell parameter variations with change of temperature. Such variations are noticeable along the *b*-axis (Table 2).

Table 2
The parameters of unit cell and quantitative analysis for hexacelsian and celsian phase in thermal treated sample HC_{Ca} (temperature range 1100–1500 °C).

T (°C)	Hexacelsian phase, HC/space group $P\bar{3}c1$			
	a (Å)	*c* (Å)	*V* (Å^3)	Content (%)
1100	5.29(1)	15.57(1)	378.2(2)	100
1200	5.29(1)	15.57(2)	377.5(2)	100
1300	5.29(2)	15.56(2)	377.5(1)	90.2
1350	5.29(2)	15.56(2)	377.5(1)	85.4
1375	5.30(2)	15.56(2)	377.3(2)	54.7
1400	5.27(1)	15.56(1)	377.0(1)	16.4
1420	5.27(1)	15.56(2)	377.0(1)	4.6
	Celsian phase, MC/space group *I*2/*c*			
	a (Å)	*b* (Å)	*c* (Å)	*V* (Å^3)	Content (%)
1300	8.60(1)	13.00(2)	14.36(1)	1458.2(1)	9.8
1350	8.58(2)	13.07(1)	14.36(1)	1462.2(1)	14.6
1375	8.60(1)	13.06(2)	14.38(2)	1466.2(2)	45.3
1400	8.60(1)	13.08(1)	14.38(1)	1463.9(1)	83.6
1420	8.61(2)	13.04(1)	14.38(2)	1463.9(2)	95.4
1450	8.62(2)	13.05(2)	14.38(1)	1466.9(1)	99.3
1500	8.62(1)	13.05(1)	14.40(2)	1469.9(2)	100

3.2. Crystal structure data of $Ba_{0.64}Ca_{0.32}Al_2Si_2O_8$

The crystal structure of celsian (S.P. *C*2/*m*) was refined with disorder of Al and Si over two sets of 8*j* sites [38]. The authors Newnham and Megaw confirmed the description of this structure [39]. It was shown that the structure is better described by in *I*2/*c* space group, with doubled *c* axis, *c* = 14. In the work of Skellern et al. [40], crystal structures of two barium-deficient celsians with different amount of vacancies, were solved in the *C*2/*m* space group. Determination the structure of monoclinic feldspar in which is Ca also present as extraframework cation may be difficult and are principally connected to order-disorder phenomena in aluminosilicate framework. Published examinations [41,42] showed that in the solid solution series (Ca, Sr) $Al_2Si_2O_8$, depending on temperature and degree of diffusion of Sr^{2+} and Ca^{2+} cations, it leads to the appearance of displacive $I\bar{1}$-$I2/c$ or $I2/c$-$I\bar{1}$ phase transition. Also, intermediate feldspar is characterized by satellite reflections which express as superstructure [43,44]. The superlattice structure is characterized by pairs of "*e*"-reflections in place of "*b*"-reflections and "*f*"-reflections as satellites to "*a*"-reflections [45]. The appearance of these reflections would depend of the crystal-ochemical composition of feldspar and annealing of temperature. In some cases K–Ca feldspar annealed at 1100°°C and above are probably in a high structural state since no "*e*" reflections were observed [46]. In the data set presented here, only the "*b*" type reflections were noticed. Consequently the *I*2/*c* space group was chosen. The structure of corresponding MC_{Ca} feldspar polymorph was refined starting with structural parameters published in the literature [34].

The final Rietveld refinement plot is shown in Fig. 2. Unit-cell parameters and agreement factors for the Rietveld refinement are given in Table 3.

These results clearly show that the structural model is very close to the starting one. The refined fractional atomic coordinates, atomic displacement parameters (U/Å^2), site occupation factors are listed in Table 4.

Prolonged temperature treatment of the Ba, Ca-diphyllosilicate phase induced increase of the thermal vibrations of extraframework cations along 6_3 axes. At critical temperatures,

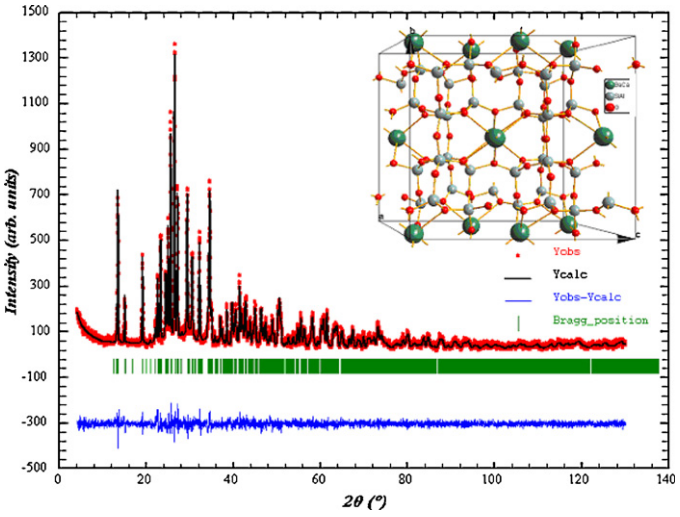

Fig. 2. The observed (circles), calculated (continuous line) and difference powder diffraction profiles for MC_{Ca} phase and the crystal structure of Ba, Ca celsian.

thermal vibrations of extraframework cations result in extreme elongations along 6_3 axes with its probable penetration inside the empty space of hexagonal prisms (D6R unit) [47]. The coordination number of M^{2+} cations in hexacelsian CN = 6 + 6 with $\bar{3}m$ local symmetry, changed into CN = 7 + 2 with m local symmetry in celsian.

The occupation factor for Ba^{2+}/Ca^{2+} was refined (Table 4). From the refined value, it can be seen that Ba, Ca feldspar was characterized with vacancies in Ba^{2+}/Ca^{2+} positions. The bond distances between oxygen anions and Ba/Ca cations are given in Table 5.

The mean Ba–O distance is longer than distance calculated from the sum of the ionic radii ~2.80 Å [48]. Griffen [34] and Newnham [39] calculated the Ba–O distance to be 2.923 and 2.920 Å respectively. Skellern et al. [40] showed that the mean Ba–O distance in the two vacant celsians was shorter for the sample with the smaller number of vacancies. Based on literature data [42], longer Sr–O distances in Sr feldspars are expected because of the lower positive charge at the partially vacant Sr site. The average bond length Ba–O in Ba, Ca feldspar is 2.928 Å. This is probably due to the presence of the Ca cations in the vacant structure.

Table 3
Unit cell parameters and agreement factors for MC_{Ca} phase.

Parameter	
a (Å)	8.6307(4)
b (Å)	13.052(4)
c (Å)	14.401(4)
β (°)	114.90(3)
V (Å^3)	1471.41(2)
R_p	17.8
R_{wp}	20.9
R_{exp}	17.63
R_B	4.58
R_F	3.12
Ch_2	1.41

Table 4
The final atomic coordinates, atomic displacement parameters (U/Å^2) and site occupation factors (occ.).

Atom	x	y	z	U	Occ.
$Ba_{(0\ 0\ 0\ 0)}$	0.283(2)	−0.00377	0.065(2)	0.27(3)	0.84(9)
$Ca_{(0\ 0\ 0\ 0)}$	0.283(2)	−0.00377	0.065(2)	0.27(3)	0.137(9)
$T_{1(0\ 0\ 0\ 0)}$	0.012(2)	0.189(2)	0.106(1)	1.07(3)	0.5
$T_{1(0\ z\ 0\ 0)}$	0.005(2)	0.178(3)	0.621(2)	1.25(3)	0.5
$T_{2(0\ 0\ 0\ 0)}$	0.718(1)	0.124(2)	0.176(2)	1.82(3)	0.5
$T_{2(0\ z\ 0\ 0)}$	0.692(2)	0.116(2)	0.668(1)	0.78(4)	0.5
$O_{A1(0\ 0\ 0\ 0)}$	0.0006(3)	0.140(1)	−0.002(1)	2.33(4)	1.0
$O_{A2(0\ 0\ 0\ 0)}$	0.633(3)	0.007(1)	0.144(1)	0.52(3)	1.0
$O_{Bo(0\ 0\ 0\ 0)}$	0.836(3)	0.150(2)	0.114(2)	0.58(2)	1.0
$O_{Bz(0\ z\ 0\ 0)}$	0.812(3)	0.127(2)	0.607(2)	0.96(2)	1.0
$O_{Co(0\ 0\ 0\ 0)}$	0.011(2)	0.320(1)	0.112(2)	3.61(2)	1.0
$O_{Cz(0\ z\ 0\ 0)}$	0.029(2)	0.304(1)	0.631(2)	0.42(5)	1.0
$O_{Do(0\ 0\ 0\ 0)}$	0.186(3)	0.128(2)	0.190 (1)	1.43(5)	1.0
$O_{Dz(0\ z\ 0\ 0)}$	0.191(3)	0.126(2)	0.699 (1)	5.02(2)	1.0

In Ba, Ca, feldspar with an Si:Al ratio of 1:1, an ordered configuration of alternating AlO_4 and SiO_4 tetrahedra is expected. The average distances $\langle T_1(0\ 0\ 0\ 0)–O\rangle$ and $\langle T_2(0\ z\ 0\ 0)–O\rangle$ were 1.658, 1.666 Å and the bond distances $\langle T_2(0\ 0\ 0\ 0)–O\rangle$ and $\langle T_1(0\ z\ 0\ 0)–O\rangle$ were 1.687, 1.70 Å. These values confirmed the ordering distribution of the Si/Al in structure of the Ba, Ca-feldspar.

In general, it could be concluded that the Rietveld structure refinement analysis of MC_{Ca} polymorph confirmed the incorporation of Ca^{2+} cations into the MC crystal lattice i.e. MC_{Ca} phase succeeded the chemical composition of its HC_{Ca} polymorph.

3.3. SEM/EDX and size/strain analysis

The crystal morphology of initial hexacelsian (HC) is given in Fig. 3(a–d).

Initial HC sample with well-developed isometric crystal forms are presented in Fig. 3a. Observed isometric forms of HC phase remain stable during the process of ion exchange (Ca^{2+} for Ba^{2+}) (Fig. 3b). Just after heating at 1420 °C for 1 h, pseudomorphic isometric crystals started to change their morphology into the rounded grain forms (Fig. 3c). A predominately glass form of newly synthesized phase MC–Ca is shown in Fig. 3d.

Table 5
Selecred interatomic distances in Å. (M represents Ba or Ca).

Distance (Å)	
$M–O_{A1}(0\ 0\ 0\ 0)$	2.822 (2)
$M–O_{A1}(0\ 0\ 0\ c)$	2.886 (2)
$M–O_{A2}(0\ 0\ 0\ 0)$	2.636 (1)
$M–O_{Bo}(0\ 0\ 0\ 0)$	2.924 (1)
$M–O_{Bz}(0\ z\ 0\ 0)$	2.946 (2)
$M–O_{Co}(0\ 0\ 0\ 0)$	3.142 (2)
$M–O_{Cz}(0\ z\ 0\ 0)$	3.116 (1)
$M–O_{Do}(0\ 0\ 0\ 0)$	2.917 (2)
$M–O_{Dz}(0\ z\ 0\ 0)$	2.904 (2)
$\langle M^{2+}–O\rangle$	2.928

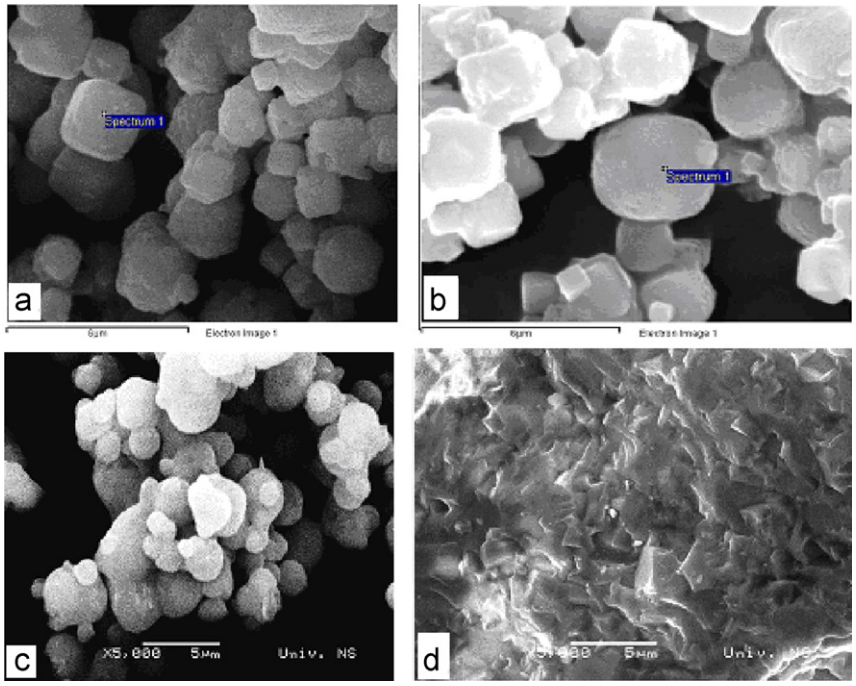

Fig. 3. Scanning electron images samples of (a) initial HC, (b) ion exchange HC_{Ca}, (c) HC_{Ca} annaled at temperature 1420 °C/1 h, and (d) MC_{Ca} phase at temperature 1500 °C/1 h.

Microstructural parameters in celsian were obtained using different methods: Warren–Averbach and simplified integral breadth method. The results of micro-strain and size parameters, for surface-weighted $\langle D_S \rangle$ and volume-weighted $\langle D_V \rangle$ are showed in Table 6. The volume-averaged domain sizes evaluated from the simplified integral-breadth method in the approximation of Cauchy–Cauchy $\langle D \rangle_{CC,}$ Cauchy–Gauss $\langle D \rangle_{CG}$, and Gauss–Gauss $\langle D \rangle_{GG}$ distribution of crystallites and strains are also given. The upper limits of strain from the simplified integral-breadth methods in the approximate Cauchy–Cauchy $\langle \varepsilon^2 \rangle^{1/2}{}_{CC,}$ Cauchy–Gauss $\langle \varepsilon^2 \rangle^{1/2}{}_{CG}$ and Gauss–Gauss $\langle \varepsilon^2 \rangle^{1/2}{}_{GG}$ distribution of crystallites and strains are also shown.The crystallite size and strain parameters, measured in the direction [0 0 *l*] [*h h* 0] [0 *k* 0] increase with temperature, according to Warren–Averbach method. Surface-weighted $\langle D_S \rangle$ and volume-weighted $\langle D_V \rangle$ crystallite size parameters in the [0 0 *l*] direction have the smallest values. The graphic presentation of the strain/size microstructural parameters are presented the in Figs. 4–6.

Table 6
The microstructure parameters calculated from the XRPD data according to the Warren–Averbach and simplifiede integral breadths method for sample HC_{Ca} annealed at temperature 1420 and 1500 °C/1 h.

Temperature (1420 °C/1 h)			Temperature, 1500 °C/1 h	
h k l	0 0 *l*	0 *k* 0	0 0 *l*	0 *k* 0
Warren–Averbach methods				
a'_3 (Å)	12.6	12.5	12.2	18.2
$\langle D_S \rangle$ (Å)	174 ± 0	284 ± 4	221 ± 2	365 ± 5
$\langle D_V \rangle$ (Å)	253 ± 1	381 ± 4.	287 ± 2	449 ± 4.
$\langle \varepsilon^2 \rangle^{1/2}{}_{\langle D \rangle S/2} \times 10^3$	0.9 ± 0.01	1.5 ± 0.02	1.4 ± 1.76	1.3 ± 1.5
$\langle \varepsilon^2 \rangle^{1/2}{}_{\langle D \rangle V/2} \times 10^3$	0.9 ± 0.02	1.4 ± 0.01	1.3 ± 1.52	1.3 ± 1.4
$\langle \varepsilon^2 \rangle^{1/2}{}_{a'3} \times 10^3$	0.2 ± 0.09	5 ± 0.061	2.9 ± 2.8	2.5 ± 5.8
$\langle \varepsilon^2 \rangle^{1/2}{}_{Gauss} \times 10^3$	0.9 ± 0.01	0.5 ± 0.02	1.1 ± 1.06	1.0 ± 1.2
Simplified integral-breadth methods				
$\langle D \rangle_{CC}$ (Å)	269	469	333	477
$\langle D \rangle_{CG}$ (Å)	253	402	292	457
$\langle D \rangle_{GG}$ (Å)	252	394	288	498
$\langle \varepsilon^2 \rangle^{1/2}{}_{CC} \times 10^3$	0.60	1.08	1.2	1.39
$\langle \varepsilon^2 \rangle^{1/2}{}_{CG} \times 10^3$	1.12	1.83	1.67	1.52
$\langle \varepsilon^2 \rangle^{1/2}{}_{GG} \times 10^3$	1.53	2.31	2.14	1.94
FullProf				
	h k l	*h k l*		
Average apparent size (Å)	674(2)	1094(2)		
Average mixing strain × 10^3 (Å)	1.513(5)	2.50		

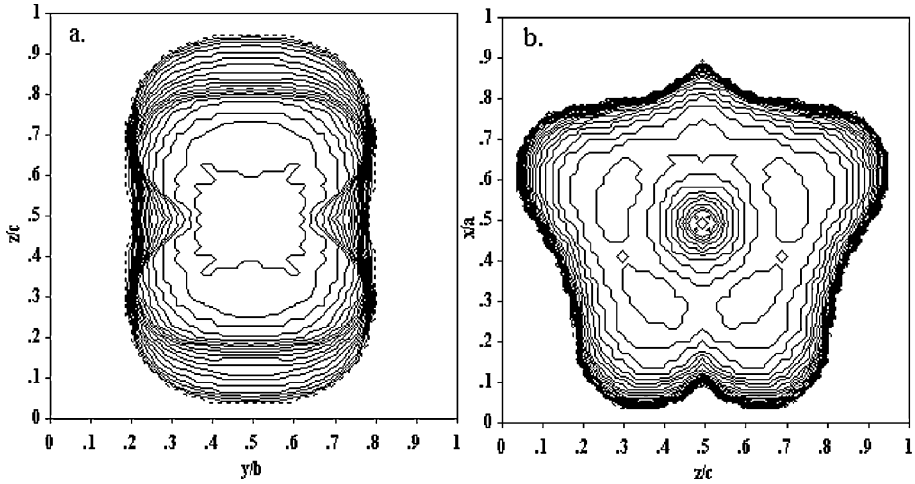

Fig. 4. The three-dimensional representation of strain of sample heating in temperature 1420 °C (a) projection in plane *c*/*b* and (b) projection in plane *c*/*a*.

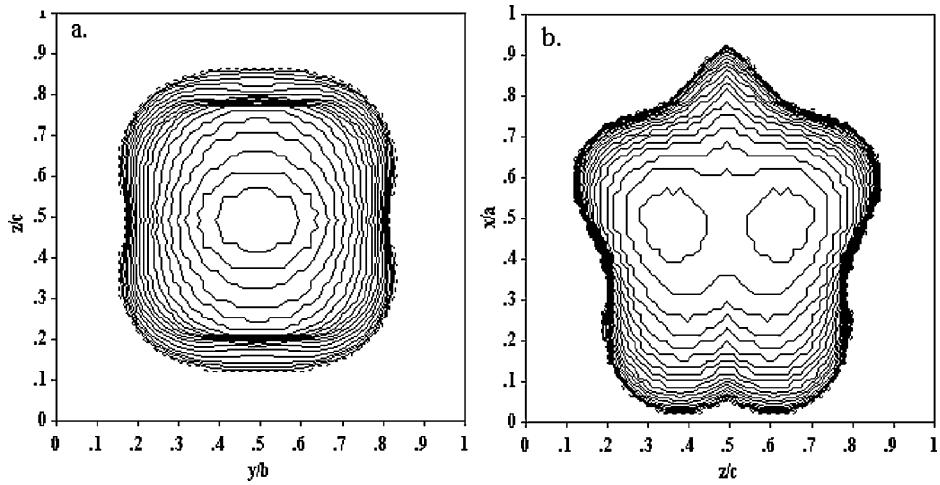

Fig. 5. The three-dimensional representation of strain of sample heating in temperature 1500 °C (a) projection in plane *c*/*b* and (b) projection in plane *c*/*a*.

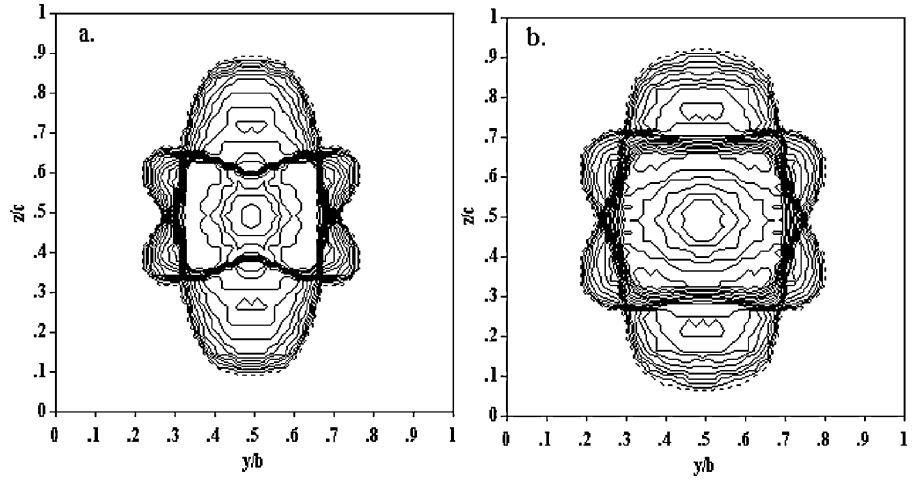

Fig. 6. The three-dimensional representation of size of sample heating in temperature (a) 1420 °C projection in plane *c*/*b* and (b) 1500 °C projection in plane *c*/*b*.

The values of the volume-averaged domain sizes $\langle D\rangle_{CC}$, $\langle D\rangle_{CG}$, and distribution of the crystallites and strains $\langle D\rangle_{GG}$ show an increase of its value in the direction [0 k 0].

4. Conclusion

This study deals with possibility of Ba, Ca celsian ceramics synthesis by using ion-exchanged hexacelsian. The procedure involves ion-exchanged hexacelsian with Ca^{2+} in autoclave at 170 °C for 7 days. The partially ion exchanged diphyllosilicate has following chemical composition $Ba_{0.64}Ca_{0.32}Al_2Si_2O_8$. The newly synthesized materials (Ba, Ca-hexacelsian HC_{Ca}) are annealed up to 1500 °C for 1 h following its structural transformation to feldspar phase using X-ray powder diffraction analysis. The XRD investigation confirmed that the HC_{Ca} compound started polymorphous transformation into MC_{Ca} feldspar at 1300 °C after 1 h. The results of XRD quantitative analysis of thermally treated HC_{Ca}, at 1420 °C for 1 h, showed presence of celsian phase in amount to 87.8%. The HC → MC transformation process is completed at 1500 °C/1 h. The crystal structure of Ba, Ca-feldspar was refined with following agreement factors: $R_p = 17.8$, $R_{wp} = 20.9$, $R(F) = 3.12$, $R(B) = 4.58$, $Ch_2 = 1.41$ for $I2/c$. Presence of Ca^{2+} in celsian did not change the structure significantly.

Acknowledgments

The authors are grateful for financial support of the Ministry of Science of the Republic Serbia (project number: III-45012).

References

[1] J.V. Smith, Feldspar Minerals I, Crystal Structures and Physical Properties, Springer, Berlin, 1974.
[2] H.C. Lin, W.R. Foster, Studies in the system BaO–Al_2O_3–SiO_2: I. The polymorphism of celsian, Am. Mineral. 53 (1968) 134–144.
[3] C.E. Semler, W.R. Foster, Studies in the system BaO–Al_2O_3–SiO_2: IV The system celsian-mulit, J. Am. Ceram. Soc. 52 (1969) 670–679.
[4] B. Yoshiki, K. Matsumoto, High-temperature modification of barium feldspar, J. Am. Ceram. Soc. 34 (9) (1951) 283–286.
[5] Y. Tabira, R.L. Withers, Y. Takéuchi, F. Marumo, Structured diffuse scattering displacive flexibility and polymorphism in Ba-hexacelsian, Phys. Chem. Miner. 27 (2000) 194–202.
[6] C.A. Sorrell, Solid-state formation of barium strontium and lead feldspars in clay–sulfate mixtures, Am. Mineral. 47 (1962) 291–309.
[7] C.H. Drummond, W.E. Lee, N.P. Bansal, M.J. Hyatt, Crystallization of a barium aluminosilicate glass, Ceram. Eng. Sci. Proc. 10 (1989) 1485–1502.
[8] M.J. Hyatt, N.P. Bansal, Crystal growth kinetics in BaO Al_2O_3 $2SiO_2$ and SrO Al_2O_3 $2SiO_2$ glasses, J. Mater. Sci. 31 (1996) 172–184.
[9] G. Dell'Agli, C. Ferone, M.C. Mascolo, M. Pansini, Thermal transformation of Ba-exchanged A and X zeolites into monoclinic celsian, Solid State Ionics 127 (2000) 309–317.
[10] B. Hoghooghi, J. McKittrik, C. Buttler, P. Desh, Synthesis of celsian ceramics from zeolite precursors, J. Non Cryst. Solids 170 (1994) 303–307.
[11] S. Esposito, C. Ferone, M. Pansini, L. Bonaccorsi, E. Proverbio, Comparative study of the thermal transformation of Ba-exchanged zeolites A, X and LSX to celsian, J. Eur. Ceram. Soc. 24 (2004) 2689–2697.
[12] R. Dimitrijević, V. Dondur, A. Kremenović, Thermally induced phase transformation of Ca-exchanged LTA and FAU zeolite frameworks: rietveld refinement of the hexagonal $CaAl_2Si_2O_8$ diphyllosilicate structure, Zeolites 16 (1996) 294–300.
[13] Ph. Colomban, H. Courret, F. Romain, G. Gouadec, Sol–gel-prepared pure and lithium-doped hexacelsian polymorphs: An infrared, Raman, and thermal expansion study of the beta-phase stabilization by frozen short-range disorder, J. Am. Ceram. Soc. 83 (12) (2000) 2974–2982.
[14] M. Chen, P. James, W. Lee, Synthesis of monoclinic celsian from seeded alkoxide gels, J. Sol Gel Sci. 1 (1994) 99–111.
[15] B. Hoghooghi, J. McKittrick, E. Helsel, O. Lopez, Microstructural development densification and hot pressing of celsian ceramics from ion exchanged zeolite precursors, J. Am. Ceram. Soc. 81 (4) (1998) 845–852.
[16] C. Ferone, S. Esposito, G. Dell'Agli, M. Pansini, Role of Li in the low temperature synthesis of monoclinic celsian from (Ba, Li)-exchanged zeolite—a precursor, Solid State Sci. 7 (2005) 1406–1414.
[17] K.T. Lee, P.B. Aswath, Kinetics of the hexacelsian to celsian transformation in barium aluminosilicates doped with CaO, Int. J. Inorg. Mater. 3 (2001) 687–692.
[18] K.T. Lee, P.B. Aswath, Role of mineralizers on the hexacelsian to celsian transformation in the barium aluminosilicate (BAS) system, Mater. Sci. Eng. A 352 (2003) 1–7.
[19] V. Dondur, R. Dimitrijevic, A. Kremenovic, L.J. Damjanovic, M. Kicanovic, H.M. Cheong, S. Macura, Phase transformation of hexacelsians doped with Li, Na and Ca, Mater. Sci. Forum 494 (2005) 107–112.
[20] V. Dondur, R. Dimitrijevic, A. Kremenovic, L.J. Damjanovic, N. Romčević, S. Macura, The lithium- and sodium-ehanced transformation of Ba-exchanged zeolite LTA into celsian phase, J. Phys. Chem. Solids 69 (2008) 2827–2832.
[21] F. Andreola, M. Romagnoli, C. Siligardi, T. Manfredini, C. Ferone, M. Pansini, Densification and crystallization of Ba-exchanged zeolite A powders, Ceram. Int. 34 (2008) 543–549.
[22] E. Bruno, G. Gazzoni, On the system $Ba[Al_2Si_2O_8]$–$Ca[Al_2Si_2O_8]$. I. Ca–Ba substitution in polymorphic modifications of $BaAl_2Si_2O_8$, Contrib. Mineral. Petrol. 25 (1970) 144–152.
[23] M. Macek Krzmanc, M. Valant, D. Suvorov, The synthesis and microwave dielectric properties of $Sr_xBa_{1-x}Al_2Si_2O_8$ and $Ca_yBa_{1-y}Al_2Si_2O_8$ ceramics, J. Eur. Ceram. Soc. 27 (2007) 1181–1185.
[24] A. Kremenovic, P. Norby, R. Dimitrijevic, V. Dondur, High-temperature synchrotron powder diffraction investigation of thermal expansion, strain and microstructure for the co-elastic alpha⟨−⟩beta hexacelsian transition, Phase Transitions 77 (2004) 955–987.
[25] W. Meier, D. Olson, Atlas of Zeolite Structure Types, Structure Commission of the IZA, Juris, Zurich, 1978.
[26] A. Dyer, in: H. Robson (Ed.), Verified Syntheses of Zeolitic Materials, 2001, 67–68.
[27] W. Kraus, G. Nolze, Powder cell – a program for the representation and manipulation of crystal structures and calculation of the resulting X-ray powder patterns, J. Appl. Crystallogr. 29 (1996) 301–303.
[28] FullProf Computer Program, 1998 Available from: ftp://charybde.saclay.cea.fr/pub/divers/fullprof.98/windows/winfp98.zip.
[29] D. Louër, J.I. Langford, Peak shape and resolution in conventional diffractometry with monochromatic X-rays, J. Appl. Crystallogr. 21 (1988) 430–437.
[30] D. Balzar, Profile fitting of X-ray diffraction lines and Fourier analysis of broadening, J. Appl. Crystallogr. 25 (1992) 559–570.
[31] D. Balzar, X-ray diffraction line broadening: modelling and applications to high-T_c superconductors, J. Res. Natl. Inst. Stand. Technol. 98 (1993) 321–353.
[32] B. Antic, A. Kremenovic, A. Nikolic, M. Stoiljkovic, Cation distribution and size-strain microstructure analysis in ultrafine Zn–Mn ferrites obtained from acetylacetonato complexes, J. Phys. Chem. B 108 (2004) 12646.
[33] A. Kremenovic, B. Antic, V. Spasojevic, M. Vucinic-Vasic, Z. Jaglicic, J. Pirnat, Z. Trontelj, XRPD line brodening analysis and magnetism of interacting ferrite naniparticles obtained from acetylacetonato complexes, J. Phys. Condens. Matter 17 (2005) 4285–4299.
[34] D.A. Griffen, P.H. Ribbe, Refinement of the crystal structure of celsian, Am. Mineral. 61 (1976) 414–418.

[35] T. Matsumoto, Y. Goto, Synthesis of monoclinic celsian from Ba-exchanged zeolite A, J. Ceram. Soc. Jpn. 110 (2002) 163–166.
[36] C. Ferone, G. Dell'Agli, M.C. Mascolo, M. Pansini, New insight into the thermal transformation of barium-exchanged zeolite A to celsian, Chem. Mater. 14 (2002) 797–803.
[37] A. Aronne, S. Esposito, C. Ferone, M. Pansini, P. Pernice, FTIR study of the thermal transformation of barium-exchanged zeolite A to celsian, J. Mater. Chem. 12 (2002) 3039–3045.
[38] W.H. Taylor, J.A. Darbyshire, H. Strunz, An X-ray investigation of the feldspars, Z. Kristallogr. 87 (1934) 464–466.
[39] R.E. Newnham, H.D. Megaw, The crystal structure of celsian (Barium Felspar), Acta Crystallogr. 13 (1960) 303–312.
[40] M.G. Skellern, R.A. Howie, E.E. Lachowski, J.M.S. Skakle, Barium-deficient celsian, $Ba_{1-x}Al_{2-2x}Si_{2+2x}O_8$ ($x = 0.20$ or 0.06), Acta Crystallogr. C 59 (2003) 11–14.
[41] M. Tribaudino, P. Benna, E. Bruno, *I*1-*I*2/*c* phase transition in alkaline-earth feldspars: Evidence from TEM observations of Sr-rich feldspars along the $CaAl_2Si_2O_8$–$SrAl_2Si_2O_8$ join, Am. Mineral. 80 (1995) 907–915.
[42] G. Chiari, M. Calleri, E. Bruno, The structure of partially disorder, synthetic strontium feldspar, Am. Mineral. 60 (1975) 111–119.
[43] Y. Nakajima, N. Morimoto, M. Kitamura, The superstructure of plagioclase feldspar, Phys. Chem. Miner. 1 (1977) 213–225.
[44] H.R. Wenk, Ordering of the intermediate plagioclase structure during heting, Am. Mineral. 63 (1978) 132–135.
[45] M.W. Roberts, J.M. Thomas, A.C. McLaren, Defects and Microstructures in feldspars,, Chem. Phys. Solids Surf. 7 (1978) 1–30.
[46] S. Mahlburg Kay, Exsolution in potassium–calcium feldspars: experimental evidence and relationship to antiperthites and Bøggild lamellae, Am. Mineral. 63 (1978) 136–142.
[47] R. Dimitrijevic, A. Kremenovic, V. Dondur, M. Tomasevic-Canovic, M. Mitrovic, Thermally induced conversion of Sr-exchanged LTA- and FAU-framework zeolites. Syntheses, characterization and polymorphism of ordered and disordered $Sr_{1-x}Al_{2-2x}Si_{2þ2x}O_8$) diphyllosilicate and feldspar phases, J. Phys. Chem. B 101 (1997) 3931–3936.
[48] R.D. Shannon, C.T. Prewitt, Effective ionic radii in oxides and fluorides, Acta Crystallogr. B 25 (1969) 925–945.